Original Paper

Dynamics of mobile ions in glass – What do conductivity spectra tell us?

Klaus Funke, Cornelia Cramer and Bernhard Roling

Institut für Physikalische Chemie and Sonderforschungsbereich 458 (DFG), Westfälische Wilhelms-Universität Münster, Münster (Germany)

Dedicated to Professor Malcolm D. Ingram on the occasion of his 60th birthday

In glassy electrolytes, the diffusive motion of the mobile ions consists of thermally activated hops from site to site. Beyond this statement, little is known about the microscopic dynamics of ionic transport in glass, the problems originating mainly from the lack of long-range order. An important step forward has been made recently by employing the technique of conductivity spectroscopy in a frequency range that covers about fourteen decades, extending up to the far infrared. This particular experimental tool acts as a "microscope in time" resolving hopping processes down to the sub-picosecond time regime. The power of the method is exemplified for the case of a lithium-ion conducting lithium bromide–lithium borate glass, which is representative in many respects. Among the results obtained is the frequent occurrence of correlated back-and-forth hopping processes as well as the finding that ions have preferences for optimally configured sites which play the role of stepping stones for translational diffusion.

Platzwechseldynamik beweglicher Ionen in einfachen anorganischen Gläsern – Was können wir aus Leitfähigkeitsspektren lernen?

In glasigen Elektrolyten besteht die Diffusionsbewegung der beweglichen Ionen aus thermisch aktivierten Sprüngen von Platz zu Platz. Darüber hinaus ist nur wenig über die mikroskopische Dynamik des Ionentransports in Glas bekannt, wobei sich die glasspezifischen Schwierigkeiten vor allem aus dem Fehlen von Fernordnung ergeben. Wesentliche Fortschritte sind in der jüngsten Vergangenheit durch den Einsatz der Leitfähigkeitsspektroskopie möglich geworden, die auf der Frequenzskala etwa vierzehn Dekaden umspannt und sich bis ins ferne Infrarot erstreckt. Die Methode hat die Wirkung eines „zeitlichen Mikroskops" und löst noch Platzwechselvorgänge im Subpicosekundenbereich auf. Die Aussagekraft des Verfahrens wird am Beispiel eines Lithiumionen leitenden Lithiumbromid–Lithiumborat-Glases demonstriert. Die erzielten Ergebnisse enthalten einerseits den Nachweis, daß es sich bei den meisten Platzwechselvorgängen um korrelierte Hin- und Rücksprünge handelt, und andererseits den Befund, daß die Ionen solche Plätze bevorzugen, die ihren Bedürfnissen optimal angepaßt sind. Ionische Sprungvorgänge über derartige Plätze sind die Elementarschritte der translatorischen Diffusion.

1. Introduction

The electrical properties of materials are determined by the dynamics of their mobile charge carriers. If the charge carriers are ions, as in many glassy materials, an applied electric field will result in an ionic current density. Electric field and current density are proportional to each other, the proportionality constant being called (specific) conductivity. In glasses, the dc conductivity is normally found to be Arrhenius-activated. This reflects the fact that it originates from thermally activated hopping processes of the mobile ions. Additional information about the ionic hopping is obtained, if the applied electric field is periodic, with frequency ν and angular frequency $\omega = 2\pi\nu$. The resulting current density has the same frequency, but a different phase. In the following, let us consider its in-phase component only. The ratio formed by this component and the applied field is called the real part of the complex conductivity and will be denoted by $\sigma(\omega)$.

Figure 1 is a log-log representation of the frequency-dependent conductivity of a sodium silicate glass as measured at different temperatures [1]. The frequency scale covered in this plot extends up to the far infrared. At Terahertz frequencies, the conductivity displays maxima which are caused by the excitation of vibrational motion. However, the most interesting feature of figure 1 is the characteristic frequency dependence of the conductivity below the vibrational regime. The very existence of this frequency dependence is in sharp contrast to the naive concept of a random hopping of the mobile

Received 3 July 2000.

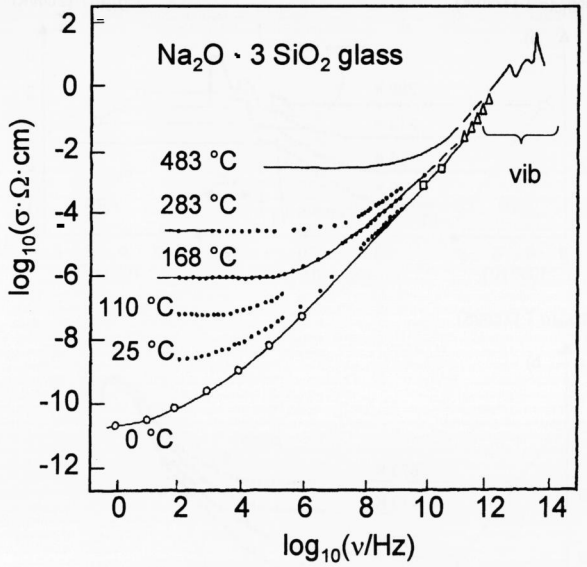

Figure 1. Frequency-dependent ionic conductivity of $Na_2O \cdot 3SiO_2$ glass [1].

ions. Random hopping would, in fact, result in a conductivity that is constant as a function of frequency. Most notably, the main features of the data shown in figure 1 are representative of the entire class of glassy electrolytes [2 to 6]. Even glasses with polaronic conduction are found to display similar behaviour [6 to 9]. Therefore, a high degree of relevance is attributed to the question "What do conductivity spectra tell us about the dynamics of the mobile ions in glass?"

Answering this question amounts to finding a way of "reading" conductivity spectra $\sigma(\omega)$. To attain this goal we must in the first place realize that the ionic movements reflected by $\sigma(\omega)$ occur in the sample permanently, irrespective of any applied electric field. This is one of the basic statements of linear response theory [10 to 12]. Using linear response theory as our guideline, we may then proceed as follows.

A time window, $\Delta t = 1/\omega$, is defined by the angular frequency ω in the sense that $\sigma(\omega)$ conveys information with resolution Δt on the time scale. In the case of ionic hopping motion, $\sigma(\omega)$ is a measure for the number of hops seen per unit time, if the time window is Δt. More explicitly, it is proportional to the number of ions found on one side of a virtual plane at time $t = t'$ and on the other at time $t = t' + \Delta t$, divided by the time interval Δt. The situation is particularly clear-cut in crystalline electrolytes like, e.g., $RbAg_4I_5$ [13]. Let us, therefore, first consider the conductivity spectrum of $RbAg_4I_5$ presented in figure 2a. In this case, the contributions to the conductivity that are due to hops and to vibrations are easily separated from each other. The contribution caused by hops of the mobile silver ions is found to increase as a function of frequency, attaining a high-frequency plateau in the millimetre-wave regime, at some

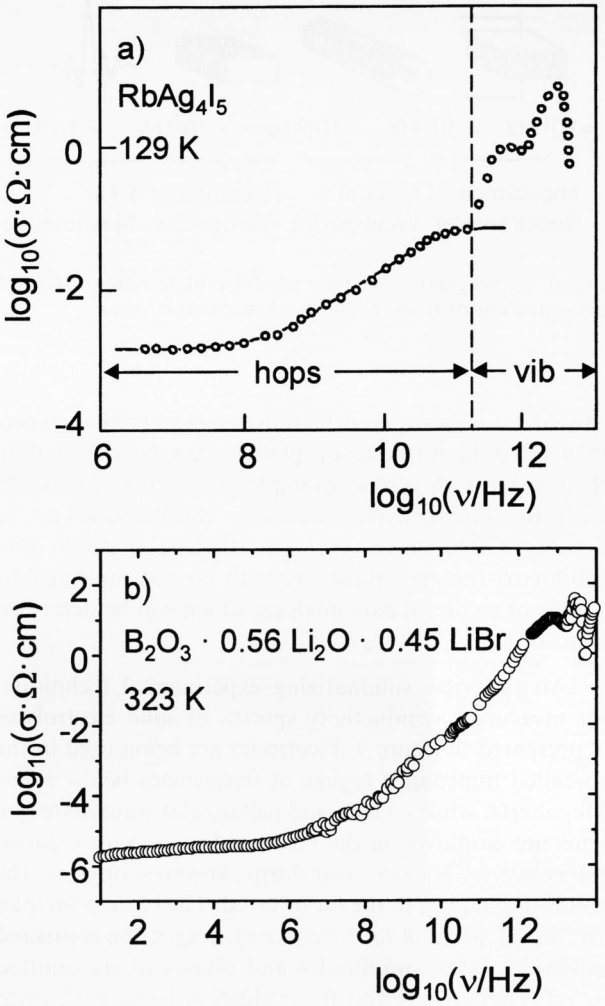

Figures 2a and b. Conductivity spectra of a) crystalline $RbAg_4I_5$ [13] and b) glassy $B_2O_3 \cdot 0.56\ Li_2O \cdot 0.45$ LiBr [2].

200 GHz. Evidently, the number of hops seen per unit time is much larger in the high-frequency plateau than in the low-frequency or dc plateau. There is a simple explanation for this observation. Most hops seen when Δt is short are no longer seen when Δt is long, since they have meanwhile been cancelled out by correlated backward hops. We may, therefore, safely conclude that there is a considerable amount of correlated forward-backward hopping in the system. In the high-frequency plateau, Δt is so short that two successive hops of one ion would not fit into this time window. As a consequence, each hop contributes to the high-frequency conductivity individually, i.e., the experiment registers all the hops occurring in the sample. On the other hand, the low-frequency conductivity plateau is due to hops that are not cancelled out by ensuing correlated backward hops. In the following, these hops will be called "successful".

In contrast to crystalline electrolytes like $RbAg_4I_5$, ion-conducting glasses do not seem to offer an obvious way of subdividing their conductivity spectra into parts

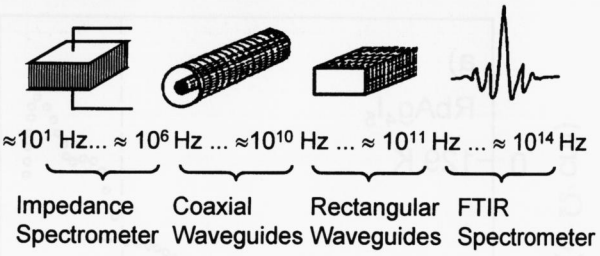

Figure 3. Schematic overview of different techniques for the measurement of frequency-dependent conductivities.

caused by hopping and vibrational movements, respectively. No high-frequency plateau can be detected in their spectra. A typical example is shown in figure 2b, with the conductivity increasing continuously up to Terahertz frequencies [2]. Nevertheless, a subdivision similar to the crystalline case can be accomplished by means of a careful data analysis, which will be described in section 3.

An overview summarizing experimental techniques for measuring conductivity spectra of solid electrolytes is presented in figure 3. Electrodes are being used in the so-called impedance regime at frequencies below a few Megahertz, while coaxial and rectangular waveguide systems are employed in the radio and microwave regimes, respectively. Fourier transform spectroscopy is the method of choice in the far infrared. The basic principles are the same in all four frequency ranges, the measured quantities being amplitudes and phases of transmitted or reflected signals and the evaluation being performed with the help of Maxwell's equations and the proper boundary conditions.

2. Conductivity spectra of inorganic glasses

Complete conductivity spectra extending up to infrared frequencies have been measured only in very few cases. Evidently, this is due to the absence of suitable high-frequency equipment in most laboratories. Complete spectra $\sigma(\omega)$ of a crystalline and a glassy electrolyte, at different temperatures, are presented and compared in figures 4a and b. In the following, the crystalline ion conductor, $RbAg_4I_5$, will be used as a reference. It displays some well-defined features which will provide a basis for understanding the more complex situation in glass.

In the crystalline electrolyte, there is an Arrhenius-type temperature dependence of the conductivity both at low frequencies and in the high-frequency plateau. This is shown in the left- and right-hand panels of figure 4a. The activation energies are, however, clearly different. The (smaller) one around 100 GHz has to be associated with individual hops, while the (larger) one at low frequencies applies for successful hops. Apparently, some additional activation energy is required for a hop to stay

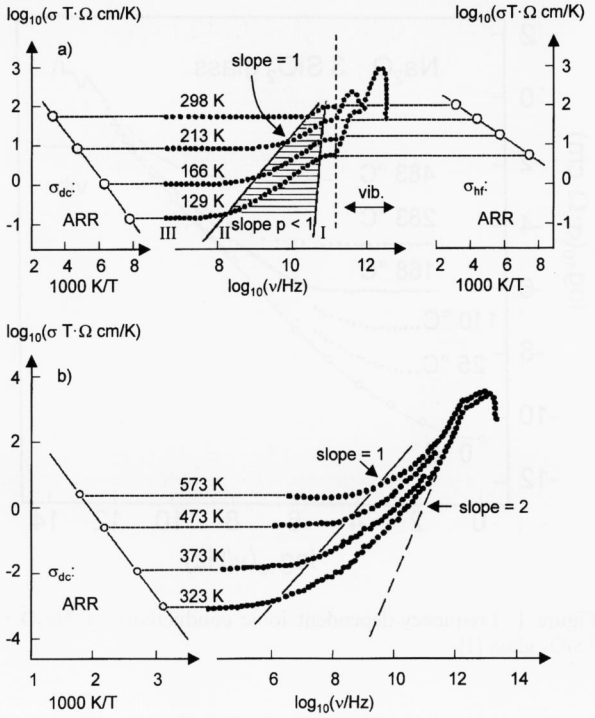

Figures 4a and b. Frequency-dependent ionic conductivities of a) crystalline $RbAg_4I_5$ [13] and b) glassy B_2O_3 · 0.56 Li_2O : 0.45 LiBr [2] at various temperatures.

successful. Between dc and the high-frequency plateau, the conductivity is frequency-dependent (dispersive) within a triangular area. In the log-log representation of figure 4a, the onset of the dispersion is found to follow a straight line with a slope of one. Shifting the conductivity isotherms along this line makes their low-frequency parts collapse in a universal curve. This is called the time-temperature superposition principle. Its validity proves that with increasing temperature ionic transport becomes more pronounced simply because the underlying transport processes become faster, while there is no indication for a change in mechanism.

Comparing the set of conductivity isotherms of the lithium-ion conducting glass of figure 4b with that of the crystalline electrolyte, we perceive analogies and differences. Once again, the temperature dependence of the dc conductivity is well described by an Arrhenius law. Furthermore, the time-temperature superposition principle is again fulfilled. On the other hand, no high-frequency plateau is detected in the millimetre-wave regime. Instead, the far-infrared conductivity is found to increase as frequency squared and then to display a broad and virtually temperature-independent shape. The latter contribution is due to vibrational motion, and the $\sigma(\omega) \propto \omega^2$ part of the conductivity spectrum is interpreted as the low-frequency flank of the lowest-lying vibrational mode.

Similar spectra have been found in silver iodide–silver borate, silver iodide–silver phosphate and silver iodide–silver selenate glasses [14 and 15].

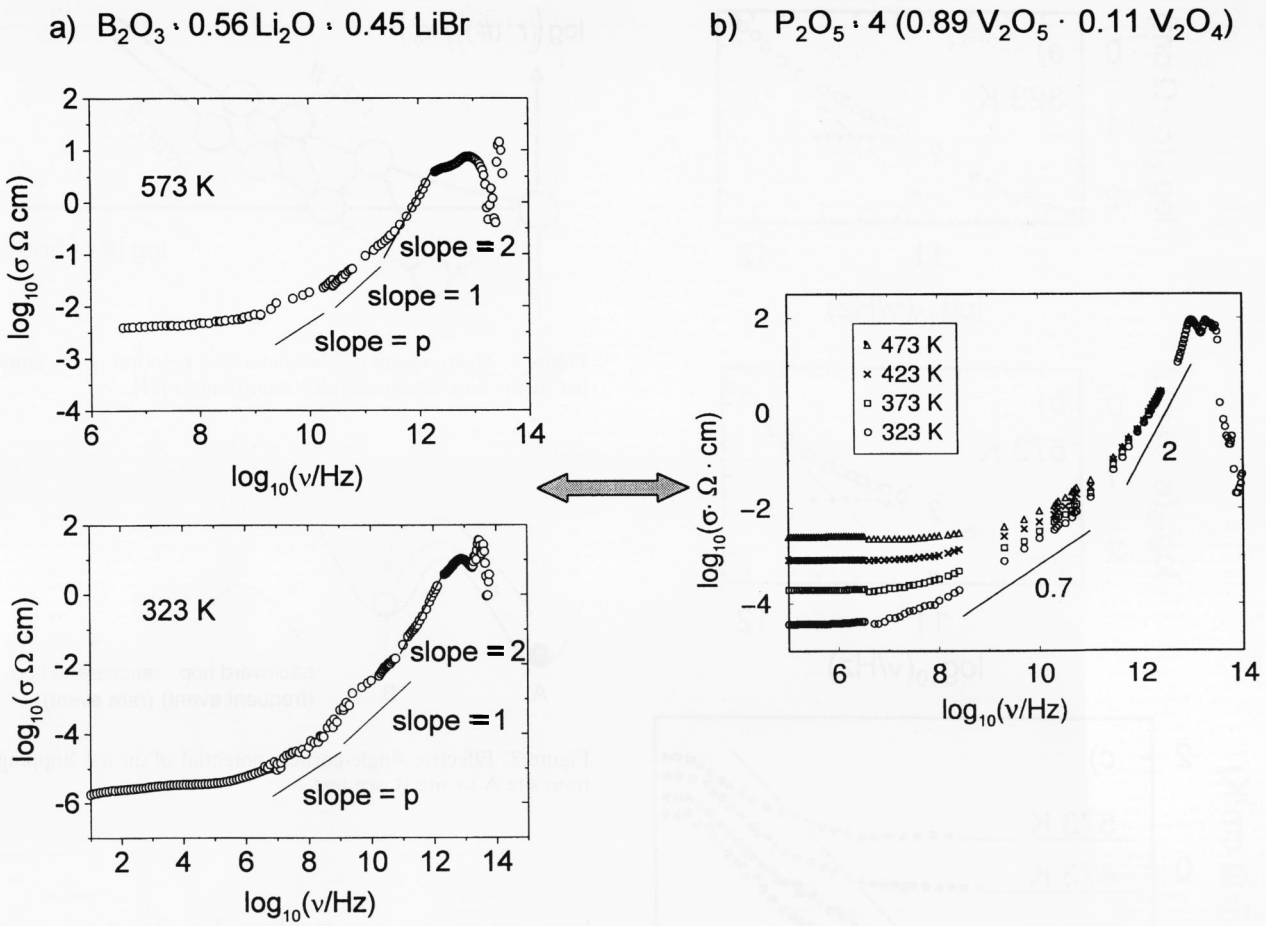

Figures 5a and b. Frequency-dependent conductivities of a) ion-conducting $B_2O_3 \cdot 0.56\,Li_2O \cdot 0.45$ LiBr [2] and b) polaron-conducting $P_2O_5 \cdot 4\,(0.89\,V_2O_5 \cdot 0.11\,V_2O_4)$ glasses [9].

It is interesting to compare the conductivity spectra of figure 4b with those of a polaron conducting glass, which is done in figures 5a and b. While the basic features are essentially similar, a remarkable difference in shape is nevertheless revealed in a log-log representation of $\sigma(\omega)$. Contrary to the ion-conducting glass, the polaronic glass, $P_2O_5 \cdot 4\,(0.89\,V_2O_5 \cdot 0.11\,V_2O_4)$, displays a less gradual increase of its frequency-dependent conductivity in the centimetre, millimetre, and sub-millimetre wave regimes, between 10 GHz and 1 THz. In the following section, this observation will be interpreted in a wider context.

3. High-frequency plateaux and relaxation processes

High-frequency plateaux of the ionic conductivity have been observed in several crystalline electrolytes ($RbAg_4I_5$ [13], Na-β-alumina [16], Na-β''-alumina [13 and 17]). Their occurrence is predicted by all hopping models and might, therefore, have been expected in ion-conducting glasses as well [18 to 20]. In glasses, however, with Brillouin zones and selection rules missing, the vibrational component of the conductivity has a broader shape and extends to lower frequencies. Therefore, we have investigated the possibility whether the high-frequency plateau might simply be swamped by the vibrational part of the spectrum. In the particular case of the lithium bromide–lithium borate glass of figure 4b, the two contributions can, in fact, be separated from each other. This is possible because the vibrational part varies exactly as frequency squared, with virtually no temperature dependence, whereas the hopping part has a different frequency dependence and varies considerably with temperature. The vibrational contribution can, therefore, be removed from the spectra and the remaining part does, indeed, display a high-frequency plateau. This is shown in figures 6a and b. A representative set of conductivity isotherms, with the vibrational contribution removed, is shown in figure 6c.

Evidently, the isotherms of figure 6c are strongly reminiscent of those of the crystalline electrolyte, see figure 4a. Again we have to conclude that the mobile ions – in this case lithium ions – perform many individual hops, most of which are of the back-and-forth kind,

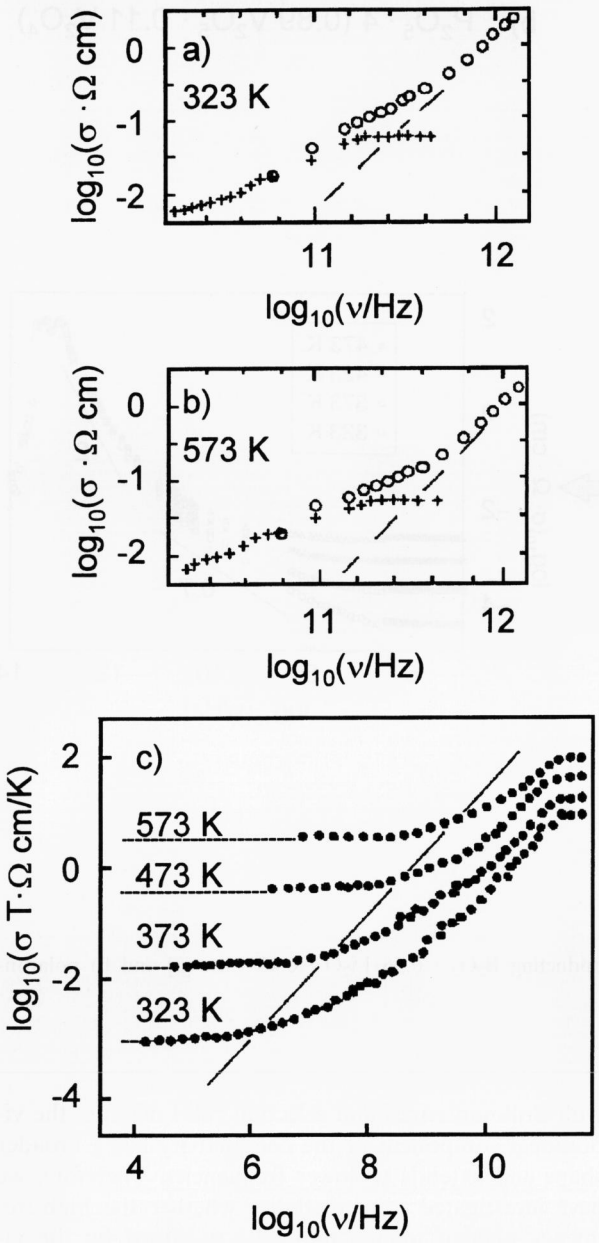

Figures 6a to c. Construction of high-frequency plateaux for glassy $B_2O_3 \cdot 0.56\ Li_2O \cdot 0.45$ LiBr (figures a and b). Conductivity component caused by the displacive and translational movement of the ions in glassy $B_2O_3 \cdot 0.56\ Li_2O \cdot 0.45$ LiBr (figure c) [2].

while only a small fraction eventually prove successful contributing to the dc conductivity and to macroscopic diffusion. The same view of the hopping motion has been obtained in Monte Carlo simulations mimicking the ion dynamics in disordered structures [21]. In figure 7, the resulting mean square displacement of the mobile ions is plotted as a function of the number of hops performed. The hopping distance is denoted by x_0. The log-log representation of figure 7 contains two distinct sets of mean square displacements, one for odd numbers of

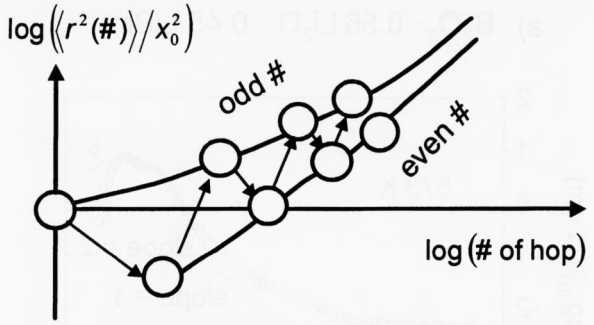

Figure 7. Mean square displacement as a function of the number of the hop. Schematic plot according to [21].

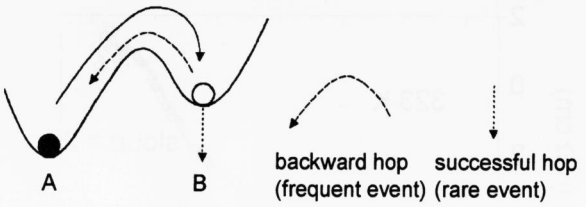

Figure 8. Effective single-particle potential of an ion hopping from site A to site B, see text.

hops and one for even numbers. The plot shows most vividly that correlated forward-backward hops are quite frequent in solid electrolytes with disordered structures.

During the past decade a model conception has been developed, which provides a physical basis for understanding the frequent occurrence of correlated forward-backward hopping processes in both crystalline and glassy electrolytes [18]. The central idea of this model is jump relaxation. In its original version, the jump relaxation model describes the hopping dynamics of the ions in a rather idealized fashion, making the following assumptions:

a) The mobile ions are all of the same kind.
b) There are many more available sites than mobile ions.
c) The available sites are all of the same kind.
d) There is no unique way of optimizing the arrangement of the ions.

The ions tend to stay at some distance from each other, since there is mutual repulsive interaction between them. Each ion is surrounded by a "cloud" of other mobile ions, much as in Debye-Hückel theory. The depth of the local potential minimum experienced by an individual ion at a particular site then depends on the momentary configuration of all its mobile neighbours. The minimum will be the deeper, the closer the ion is to the centre of the cloud, i.e., to the position where its neighbours "expect" it to be. The essential aspects are visualized in figure 8. Suppose the ion resides at position

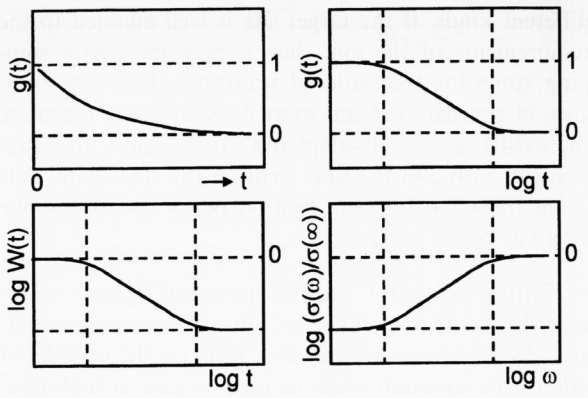

Figure 9. Central functions of the jump relaxation model [18]: mismatch function $g(t)$, time-dependent correlation factor $W(t)$ and normalized conductivity spectrum of the hopping motion, $\sigma(\omega)/\sigma(\infty)$.

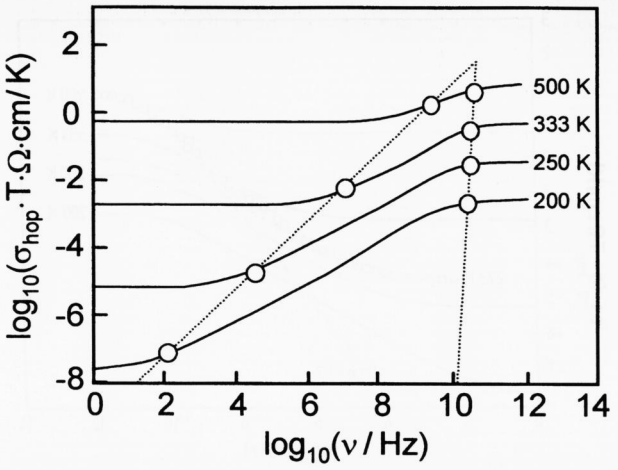

Figure 10. Conductivity spectra resulting from the jump relaxation model [18].

A, which is closer to the centre of the cloud than B. If the ion performs a hop from A to B, it will experience an energetically less favourable situation there. In other words, mismatch has been created. The system now tries to find ways to relax the mismatch. Two competing ways of mismatch relaxation can be envisaged. The ion may hop back to its original site (single-particle route) or the neighbouring ions rearrange in the course of their own hopping motion, thereby lowering the local potential at B (many-particle route). Only if, in the course of this process, a new absolute potential minimum is formed at B, the "initial forward" hop from A to B has proved successful and thus contributes to macroscopic transport.

To describe the resulting dynamics, we introduce two functions of time called $g(t)$ and $W(t)$, see figure 9. The so-called mismatch function $g(t)$ is the normalized distance between position B and the centre of the cloud of neighbouring ions. The time dependence of $g(t)$ reflects the movement of the centre of the cloud, under the condition that the ion stays at B. Approximating the effect of the neighbours on the ion with the help of a harmonic cage-effect potential, we may identify $g(t)$ with a normalized negative gradient of that potential, which is a normalized backward driving force. As shown in figure 9, this backward driving force decays with time, if the ion stays at B. The function $W(t)$ is a time-dependent correlation factor. It is the probability for the correlated backward hop from B to A not to have occurred at time t after the hop from A to B. Like $g(t)$, $W(t)$ is a decaying function of time. However, the very existence of macroscopic transport implies that $W(t)$ must stay finite at long times, approaching a non-zero value $W(\infty)$.

In section 1, $\sigma(\omega)$ was interpreted as a measure for the number of hops seen per unit time, if the time window is $\Delta t = 1/\omega$. This is exactly the average total hopping rate per ion, times the number of mobile ions, times $W(1/\omega)$. We may hence conclude that, in log-log plots, the functions $\sigma(\omega)/\sigma(\infty)$ and $W(t)$ are mirror images of each other, see figure 9. Comparison with linear response theory shows that the error made in this rough and very intuitive approach is, indeed, negligible.

Therefore, to derive $\sigma(\omega)$ we need to know $W(t)$. As $W(t)$ is intimately connected with $g(t)$, we must know both functions simultaneously. In a formal treatment, the two functions can be obtained as soon as two independent equations are available that connect them. Finding a suitable pair of equations is the essential step in modelling. The pair of equations used in the jump relaxation model, see below, yields sets of model conductivity isotherms like those presented in figure 10. It is quite evident that the main features of experimental spectra, see figure 4a, are well reproduced.

The two equations employed in the jump relaxation model make the following statements.

- Under the condition that the ion is still at B, the rates of relaxation via the "single-particle route" and via the "many-particle route" are balanced at all times, i.e., they are proportional to each other and decay in a synchronized fashion. In other words, the tendency for the ion to perform a correlated backward hop is at all times proportional to the tendency of its neighbours to rearrange.
- A Boltzmann Ansatz is employed to express time-dependent (backward) hopping rates in terms of time-dependent potential barriers.

The resulting model conductivity spectra, see figure 10, fulfil the following simple relation to a good approximation

$$\sigma(\omega) - \sigma(0) \propto (1 + \omega_1/\omega)^{-p}. \qquad (1)$$

Here, $p < 1$ plays the role of a power-law exponent in the dispersive regime of $\sigma(\omega)$, while ω_1 marks the transition into the high-frequency plateau.

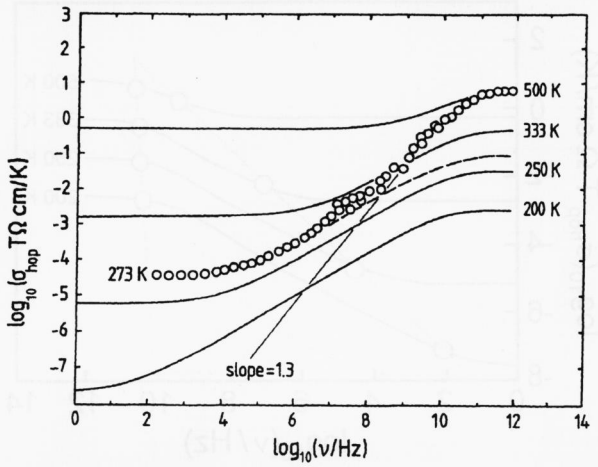

Figure 11. Conductivity spectrum of glassy $B_2O_3 \cdot 0.56\ Li_2O : 0.45$ LiBr at 273 K [2] and model spectra obtained by the jump relaxation model [18].

Comparing equation (1) with the experimental conductivity spectra of figure 4a and figure 6c, we find good agreement in the case of the crystalline electrolyte, but characteristic differences in the case of the glass. For clarity, the 273 K conductivity isotherm of the lithium bromide–lithium borate glass is reproduced in figure 11 and presented along with several isotherms obtained from equation (1). Evidently, a single power-law exponent does not suffice to describe the data. Rather, a very good fit is achieved by the equation

$$\sigma(\omega) - \sigma(0) = \alpha \cdot (1 + \omega_1/\omega)^{-0.6} + \beta \cdot (1 + \omega_1/\omega)^{-1.3}, \quad (2)$$

see figure 11.

The second term in equation (2) requires an explanation that is not provided by the jump relaxation model as outlined above. It is, however, helpful to inquire into the role the exponent p plays in the model. In doing so, we find that it equals the ratio formed by the (properly normalized) rates of mismatch relaxation along the single- and the many-particle routes. If this ratio is less than one, this means that the rate describing the tendency of the ion to perform a correlated backward hop is smaller than the rate at which its potential at site B (in units of the thermal energy, kT) is lowered as the neighbours rearrange. In this case $W(\infty)$ has a non-zero value, resulting in macroscopic transport. If, on the other hand, the ratio exceeds one, then the correlated backward hopping prevails over the lowering of the potential at B. This kind of hopping process does not contribute to the dc conductivity.

To resolve the puzzle of the two exponents in equation (2), we have to acknowledge the possibility that in a glass a mobile ion may hop into target sites of different kinds. If the target site is well adapted to the requirements of the ion, then it may serve as a stepping stone for translational transport. The very existence of translational transport does, in fact, necessitate the existence of well-adapted ("good") sites. In equation (2), $\sigma(0)$ and the first term on the right-hand side result from the hopping motion performed by mobile ions via "good" sites.

Fitting equation (2) to the spectra of figure 6 we realise that $\alpha(T)$ and $\beta(T)$ have different activation energies. As a consequence, the first term on the right-hand side of the equation tends to predominate at high temperatures, while the second term determines the high-frequency dynamics at lower temperatures. The fact that equation (2) provides a good fit for the experimental data should, however, not be misinterpreted as compelling evidence for only two kinds of target site, "good" ones and "bad" ones. An entire range of intermediate-quality sites may be present, but this is hard to decide from the spectra.

The finding of different kinds of site fits in nicely with the concept of the "dynamic structure model", which claims that translational hopping is via optimally configured sites, while less favourable sites also exist and possibly even prevail [22]. The extension of the jump relaxation model described in this section thus includes essential features of the dynamic structure model. It has, therefore, been called the "unified site relaxation model" [2 and 23].

Differentiating between "good" and "bad" target sites means that a site preference is ascribed to the ions. Ions seem to judge the quality of a site from certain properties such as size and charge distribution in its surroundings. The effect is also reflected by the drastic increase of the ionic mobility with increasing number density of mobile ions in glass. In the dynamic structure model this well-known observation is explained by the creation of more and more sites of the well-adapted, preferred kind as the number of mobile ions is increased. The model even correctly predicts the dependence of the mobility on the concentration of the mobile ions, which follows a power law.

Most remarkably, this power-law concentration dependence is not observed in the case of polaronically conducting glasses like $P_2O_5 \cdot 4$ ($0.89\ V_2O_5 \cdot 0.11\ V_2O_4$). Here, the mobile electrons (small polarons) have mobilities that do not seem to vary with their concentration [9 and 24]. Hence there is no indication of any site preference. This result is in perfect agreement with the conductivity spectra shown on the right-hand side of figure 5. In fact, these spectra are nicely fitted without any second term in equation (2), indicating that all available sites are equally well-suited to host a small polaron. In conclusion, site preference appears to be characteristic of ionic, but not of electronic charge carriers.

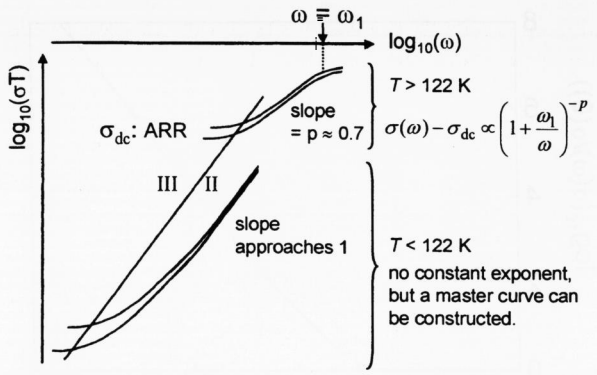

Figure 12. Sketch of the conductivity isotherms of crystalline $RbAg_4I_5$ [13] at temperatures above and below the $\beta-\gamma$ phase transition. The straight line with slope one separates the dc regime (III) from the dispersive regime (II).

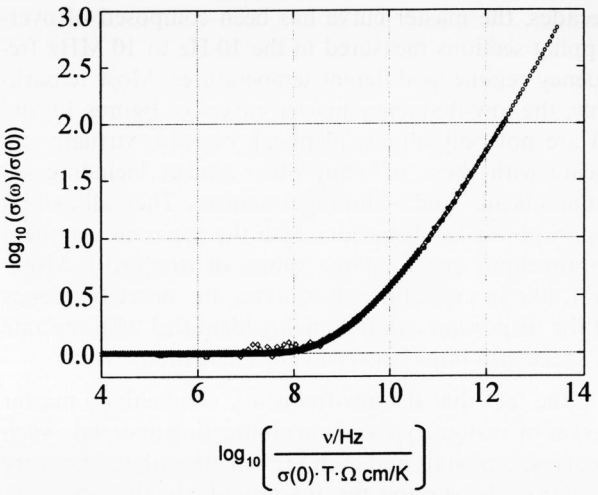

Figure 13. Low-frequency conductivity master curve of sodium borate glasses [29].

4. Low-frequency scaling of the conductivity

In the preceding section, the jump relaxation model and the resulting simple scheme of figure 10 were introduced to provide a general basis for understanding the ion dynamics in solid electrolytes. In the case of glass, deviations from this scheme were observed at radio and microwave frequencies, i.e., well above the so-called impedance regime. The deviations were traced back to properties of glass that had not been allowed for in the original model, thereby adding to our understanding of the ion dynamics. In this section, we consider another deviation from the scheme of figure 10. It is observable in the impedance regime and becomes more and more pronounced when the temperature is decreased. Interestingly, this feature is found in both crystalline and glassy electrolytes.

Figure 12 is a sketch of the effect as observed in the crystalline electrolyte $RbAg_4I_5$. While the essence of the conductivity isotherms at temperatures above the $\gamma-\beta$ phase transition at 122 K is adequately described by equation (1), see figures 4a and 10, different characteristics become apparent at lower temperatures. On the one hand, the time-temperature superposition principle is still found to be valid, which means that the low-frequency parts of the conductivity isotherms all collapse in a universal master curve, irrespective of the phase transition [25]. On the other hand, the shape of the dispersion starts to deviate from equation (1), the more so, the larger the ratio $\sigma(\omega)/\sigma(0)$ becomes. With increasing $\sigma(\omega)/\sigma(0)$, the apparent power-law exponent gradually approaches the value of one. At sufficiently low temperatures, the ratio $\sigma(\omega)/\sigma(0)$ takes on large values at any given frequency, resulting in a slope of almost one of the respective conductivity isotherm at this frequency. This effect, together with the time-temperature superposition principle, implies that the temperature dependence of the conductivity becomes very small, if the temperature is low and the frequency is held constant. As a linear frequency dependence of the conductivity is equivalent to

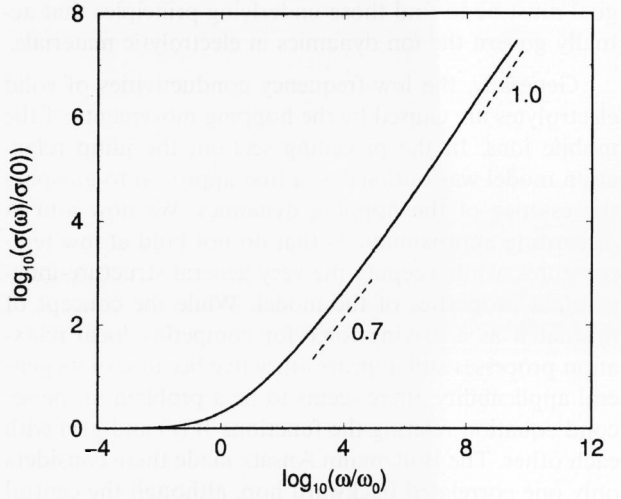

Figure 14. Low-frequency conductivity master curve of 0.3 AgI · 0.7 $AgPO_3$ [32].

an absence of any frequency dependence of the dielectric loss, the effect has been termed "nearly constant loss behaviour" [26 to 28].

The spectra of figure 12 suggest that the power law of equation (1) is no more than an approximation valid only as long as the ratio $\sigma(\omega)/\sigma(0)$ does not exceed a certain value. In a more adequate description, the power-law concept would have to be abandoned in favour of a more realistic treatment.

The distinctive features outlined in figure 12 are also found in the low-temperature, low-frequency conductivities of glassy electrolytes [29 to 32]. In figures 13 and 14 we present the examples of sodium borate [29] and silver iodide–silver phosphate glasses [30 and 32]. In the latter case, with $\sigma(\omega)/\sigma(0)$ extending over almost eight

decades, the master curve has been composed of overlapping sections measured in the 10 Hz to 10 MHz frequency regime at different temperatures. Most remarkably, the low-frequency master curves of figures 13 and 14 are not only almost identical, but also virtually coincide with those of many other glasses including sodium silicates and sodium germanates. They all exhibit a non-power-law behaviour with the apparent exponent approaching one for large values of $\sigma(\omega)/\sigma(0)$. Moreover, like in crystalline electrolytes, the onset frequency of the dispersion can be roughly identified with the rate of successful hops between equivalent sites.

The fact that the low-frequency conductivity master curves of various types of ion-conducting materials, such as glasses, crystals and even molten electrolytes, are very similar in shape raises the question of why the long-term ion dynamics of these systems should exhibit such a high degree of universality. Clearly, attempts to explain the universal shape of the master curve should refrain from making too much reference to any particular structure-related conduction mechanism. Instead, the primary goal must be to find those underlying principles that actually govern the ion dynamics in electrolytic materials.

Generally, the low-frequency conductivities of solid electrolytes are caused by the hopping movements of the mobile ions. In the preceding section, the jump relaxation model was outlined as a first approach to grasping the essence of the hopping dynamics. We now aim at discarding approximations that do not hold at low temperatures, while keeping the very general structure-independent properties of the model. While the concept of mismatch as a driving force for competing local relaxation processes still appears attractive because of its general applicability, there seems to be a problem in the second equation relating the functions $W(t)$ and $g(t)$ with each other. The Boltzmann Ansatz made there considers only one correlated backward hop, although the central ion may perform an entire series of correlated back-and-forth hops, in particular so at low temperatures, where $g(t)$ decays rather slowly. The oversimplifying Boltzmann Ansatz is, therefore, discarded and replaced by a completely different approach. The mismatch reduction at the site of the central ion is now explicitly described as resulting from hopping movements in the neighbourhood which have been induced by the mismatch itself. The rate of those hops is hence assumed to be proportional to $g(t)$. An aspect of self-consistency is then introduced by postulating that the movement of the neighbours has to be described by the same back-and-forth hopping dynamics as that of the central ion itself.

The approach sketched in the preceding paragraph has been termed "concept of mismatch and relaxation" (CMR) and may be considered an improved version of the jump relaxation model [25 and 32]. Deriving $W(t)$ and $g(t)$ from the CMR, then forming the mirror image of $W(t)$ in the log-log representation and focusing on the low-frequency part of the conductivity only, one eventually arrives at a non-power-law equation for the

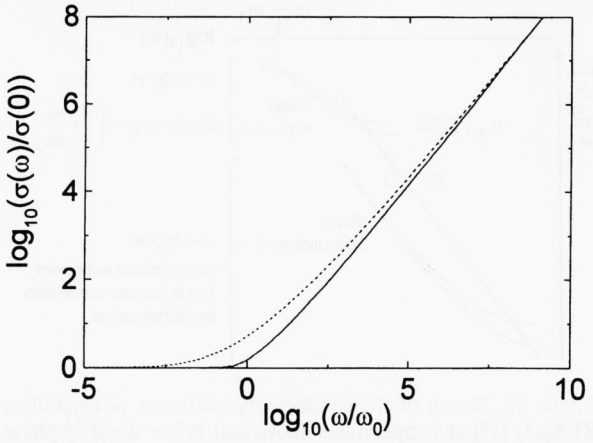

Figure 15. Comparison of the experimental low-frequency conductivity master curve of figure 14 (broken line) with the result from the CMR model (solid line) [32].

normalized function $\sigma(\omega)/\sigma(0) = f(\omega/\omega_0)$, which does not contain a single parameter and, therefore, describes the low-frequency master curve in a fixed and unique fashion, i.e.,

$$\ln(\sigma(\omega)/\sigma(0)) = E_1^{-1}(\omega_0/\omega) \,. \tag{3}$$

In equation (3), E_1^{-1} denotes the inverse function of the exponential integral E_1^{-1}, which is defined by

$$E_1(x) = \int_x^\infty \frac{\exp(-y)}{y}\,\mathrm{d}y \,, \tag{4}$$

while ω_0 marks the onset of the dispersion on the angular frequency scale.

The low-temperature, low-frequency conductivities of $RbAg_4I_5$ and other crystalline electrolytes are, in fact, perfectly well reproduced by equation (3) [25]. This is in itself an important result. However, comparing equation (3) and the low-frequency conductivity master curves of glassy materials, see figure 15, we still encounter differences. These do not concern the distinctive properties of the conductivity at large ratios of $\sigma(\omega)/\sigma(0)$, where equation (3) correctly describes the gradual transition into a linear regime. Rather, differences are found at angular frequencies around ω_0, where the onset of the dispersion is less abrupt in glass than it is according to equation (3) and in crystalline electrolytes like $RbAg_4I_5$ [12], β–AgI [33], and others.

We, therefore, conclude that the assumptions leading to equation (3) are reasonably well fulfilled in $RbAg_4I_5$ and other crystals, while the differences seen between the two master curves of figure 15 are indicative of specific properties of glass. The time-temperature superposition principle being fulfilled in glass, these properties exert the same influence on the ion dynamics at all temperatures. As temperature-independent properties are likely

to be geometrical in nature, the geometric arrangement of the available sites in glass, which is non-periodic, appears to be a good candidate for explaining the differences of figure 15. In a glassy ion conductor, different sites are differently connected with others, some of them forming little clusters, others acting rather as bottlenecks for translational diffusion. In such a configuration of sites a successful hop does, strictly speaking, not yet represent an elementary step of diffusion which, by definition, creates macroscopic transport by random repetition. Rather, an elementary step in the rigorous sense of the word will only be accomplished when the ion arrives at a site that is roughly equivalent to the previous one. Only then will the ion lose memory of its previous dynamics so that random diffusion will ensue and the dc plateau of the conductivity will be attained. Before that is achieved, however, the ion will, on a time scale of a few successful hops, experience some degree of geometrical confinement and then pass on to other sites nearby. This transient confinement effect results in a reduced dc conductivity, which is attained at lower frequencies than for a periodic arrangement of sites. Compared to crystalline electrolytes, glassy ion conductors are thus expected to show an additional gradual reduction of the conductivity as the frequency is reduced into the dc plateau regime. The effect may, therefore, well account for the specific shape of the frequency-dependent conductivity of glass seen in the onset regime of the dispersion.

5. Conclusion and outlook

There is a host of problems in glass science, most of them resulting from the lack of long-range order. Although diffraction patterns that are devoid of Bragg peaks allow statements about neighbouring shells and average distances, they do of course not provide a possibility of assigning well-defined sites to atoms and ions. Still more formidable than the problem "Where are the ions?" is, however, the other one, "How did the ions get there and what will they do next?". Answers to this demanding question can only be given with the help of experimental tools that act as "microscopes in time". Here, conductivity spectroscopy has been established as one of the most powerful techniques because it permits the study of the ion dynamics over the entire range of relevant times extending from seconds down to the subpicosecond regime. In this paper we have shown that, on the basis of ionic-conductivity spectra, relevant answers can be given to questions concerning the dynamics of the mobile ions in glass. The most striking dynamic property thus revealed is possibly the large amount of back-and-forth hopping of the ions. Secondly, the spectra clearly prove that the ions have a preference for sites that optimally meet their requirements. Thirdly, macroscopic diffusion occurs via these preferred and well-adapted sites, which play the role of stepping stones throughout the glassy network. As the temperature is varied, no change is observed in the diffusion mechanism. This conclusion is drawn from the validity of the time-temperature superposition principle. Finally, the shape of the low-frequency conductivity dispersion appears to reflect specific aspects of ion transport in glass that have their origin in the geometrical arrangement of the available sites and in locally different connectivities.

The structure and dynamics of ion-conducting glasses provide many more scientific challenges, and quite a few of them are presently being tackled using conductivity spectroscopy. These challenges include the variations of transport properties that are observed along with changes of composition. In this area, the most intriguing puzzle is probably the mixed alkali effect or, put more generally, the mixed mobile ion effect. Indications are that this effect is not simply a long-distance percolation problem. Rather, as in glasses with only one mobile species, there seems to be a continuous evolution of the dynamics with time, the effect being already present on the picosecond time scale.

*

It is a pleasure to thank Hellmut Eckert for critically reading the manuscript.

6. References

[1] Wong, J.; Angell, C. A.: Glass: Structure by spectroscopy. New York and Basel: Dekker, 1976.
[2] Cramer, C.; Funke, K.; Saatkamp, T. et al.: High-frequency conductivity plateau and ionic hopping processes in a ternary lithium borate glass. Z. Naturforsch. **50a** (1995) p. 613–623.
[3] Cramer, C.: Ion and polaron conducting glasses. Ber. Bunsenges. Phys. Chem. **100** (1996) p. 1497–1502.
[4] Cramer, C.; Funke, K.; Roling, B. et al.: Ionic and polaronic hopping in glass. Solid State Ionics **86–88** (1996) p. 481–486.
[5] Cutroni, M.; Mandanici, A.; Piccolo, A. et al.: Frequency and temperature dependence of ac conductivity of vitreous silver phosphate electrolytes. Solid State Ionics **90** (1996) p. 167–172.
[6] Pradel, A.; Taillades, G.; Ribes, M. et al.: Ion dynamics in superionic chalcogenide glasses studied in large frequency and temperature ranges. Solid State Ionics **105** (1998) p. 139–148.
[7] Summerfield, S.: Universal low-frequency behaviour in the a.c. hopping conductivity of disordered systems. Phil. Mag. B **52** (1985) p. 9–22.
[8] Elliott, S. R.: Frequency-dependent conductivity in ionically and electronically conducting amorphous solids. Solid State Ionics **70&71** (1994) p. 27–40.
[9] Roling, B.; Funke, K.: Polaronic transport in vanadium phosphate glasses. J. Non-Cryst. Solids **212** (1997) p. 1–10.
[10] Kubo, R.: Statistical-mechanical theory of irreversible processes. I. General theory and simple applications to magnetic and conduction problems. J. Phys. Soc. Japan **12** (1957) p. 570–586.
[11] Kohler, F.: The liquid state. Weinheim: Verl. Chemie, 1972.
[12] McQuarrie, D. A.: Statistical mechanics. New York: Harper Collins, 1976.

[13] Hoppe, R.; Kloidt, T.; Funke, K.: Frequency-dependent conductivities of $RbAg_4I_5$ and Na-β''-alumina from radio to FIR frequencies. Ber. Bunsenges. Phys. Chem. **95** (1991) p. 1025–1028.
[14] Cramer, C.; Buscher, M.: Complete conductivity spectra of fast ion conducting silver iodide/silver selenate glasses. Solid State Ionics **105** (1998) p. 109–120.
[15] Cramer, C.; El-Egili, K. A. I.; Gockel, J. et al.: Elementary steps of ionic motion in glasses studied by conductivity spectroscopy above and below the glass transition temperature. Solid State Ionics. In preparation.
[16] Strom, U.; Ngai, K. L.: Ac conductivity of Na-β-Al_2O_3 from 10^2 Hz to 10^{11} Hz and from 0.02 K to 600 K: a generalized treatment. Solid State Ionics **5** (1981) p. 167–170.
[17] Cramer, C.; Graeber, R.; Ingram, M. D. et al.: Complete conductivity spectra of crystalline and glassy fast ion conductors up to far infrared frequencies. Mat. Res. Soc. Symp. Proc. **369** (1995) p. 233–243.
[18] Funke, K.: Jump relaxation in solid electrolytes. Progr. Solid State Chem. **22** (1995) p. 111–195.
[19] Maass, P.; Meyer, M.; Bunde, A.: Nonstandard relaxation behavior in ionically conducting materials. Phys. Rev. B **51** (1995) p. 8164–8177.
[20] Knödler, D.; Pendzig, P.; Dieterich, W.: Transport and ac response in a model of glassy electrolytes. Solid State Ionics **70–71** (1994) p. 356–361.
[21] Maass, P.; Petersen, J.; Bunde, A. et al.: Non-Debye relaxation in structurally disordered ionic conductors: effect of Coulomb interaction. Phys. Rev.Lett. **66** (1991) p. 52–55.
[22] Bunde, A.; Ingram, M. D.; Maass, P.: The dynamic structure model for ion transport in glasses. J. Non-Cryst. Solids **172–174** (1994) p. 1222–1236.
[23] Bunde, A.; Funke, K.; Ingram, M. D.: Ion hopping processes and structural relaxation in glassy materials. Solid State Ionics **86–88** (1996) p. 1311–1317.
[24] Linsley, G. S.; Owen, A. E.; Hayatee, F. M.: Electronic conduction in vanadium phosphate glasses. J. Non-Cryst. Solids **4** (1970) p. 208–219.
[25] Funke, K.; Wilmer, D.: Concept of mismatch and relaxation derived from conductivity spectra of solid electrolytes. Mat. Res. Soc. Symp. Proc. **548** (1999) p. 403–414.
[26] Lee, W. K.; Liu, J. F.; Nowick, A. S.: Limiting behaviour of ac conductivity in ionically conducting crystals and glasses: a new universality. Phys. Rev. Lett. **67** (1991) p. 1559–1561.
[27] Nowick, A. S.; Lim, B. S.; Vaysleyb, A. V.: Nature of the ac conductivity of ionically conducting crystals and glasses. J. Non-Cryst. Solids **172–174** (1994) p. 1243–1251.
[28] Nowick, A. S.; Vaysleyb, A. V.; Liu, W.: Identification of distinctive regimes of behaviour in the ac electrical response of glasses. Solid State Ionics **105** (1998) p. 121–128.
[29] Roling, B.; Funke, K.; Happe, A. et al.: Carrier concentrations and relaxation spectroscopy: New information from scaling properties of conductivity spectra in ionically conducting glasses. Phys. Rev. Lett. **78** (1997) p. 2160–2163.
[30] Roling, B.; Ingram, M. D.; Lange, M. et al.: The role of AgI for ionic conduction in AgI-$AgPO_3$ glasses. Phys. Rev. B **56** (1997) p. 13619–13622.
[31] Roling, B.: Scaling properties of the conductivity spectra of glasses and supercooled melts. Solid State Ionics **105** (1998) p. 185–193.
[32] Funke, K.; Roling, B.; Lange, M.: Dynamics of mobile ions in crystals, glasses and melts. Solid State Ionics **105** (1998) p. 195–208.
[33] Funke, K.; Wilmer, D.; Lauxtermann, T. et al.: Creation and recombination of Frenkel defects in AgBr. Solid State Ionics **86–88** (1996) p. 141–146.

0800P003

Address of the authors:

K. Funke, C. Cramer, B. Roling
Institut für Physikalische Chemie und Sonderforschungsbereich 458
Westfälische Wilhelms-Universität Münster
Schloßplatz 4/7
D-48149 Münster